Title: Computational electrophysiology to support the mapping of coronary sinus branches for cardiac resynchronization therapy

Christian Vergara, PhD[a,*], Simone Stella, MSc[b], Massimiliano Maines, MD[c], Domenico Catanzariti, MD[c], Cristina Demattè, MD[c], Maurizio Centonze, MD[d], Fabio Nobile, PhD[e], Alfio Quarteroni, PhD[f], Maurizio Del Greco, MD[c]

[a] LABS, Dipartimento di Chimica, Materiali e Ingegneria Chimica "Giulio Natta", Politecnico di Milano, Piazza Leonardo da Vinci 32, 20233, Milan, Italy, christian.vergara@polimi.it

[b] MOX, Dipartimento di Matematica, Politecnico di Milano, Piazza Leonardo da Vinci 32, 20233, Milan, Italy, simone.stella@polimi.it

[c] Department of Cardiology, S. Maria del Carmine Hospital, corso Verona 4, 38068, Rovereto (TN), Italy, <massimiliano.maines, domenico.catanzariti, cristina.dematte,maurizio.delgreco>@apss.tn.it

[d] U.O. di Radiologia di Borgo-Pergine, Borgo Valsugana Hospital, Borgo Valsugana (TN), Italy, contendermc@gmail.com

[e] CSQI, Institute of Mathematics, École Polytechnique Fédérale de Lausanne, Route Cantonale, 1015 Lausanne, Switzerland, fabio.nobile@epfl.ch

[f] MOX, Dipartimento di Matematica, Politecnico di Milano, Piazza Leonardo da Vinci 32, 20233, Milan, Italy & Institute of Mathematics, École Polytechnique Fédérale de Lausanne, Switzerland (professor emeritus), alfio.quarteroni@polimi.it

* Corresponding author

Conflict of interest statement. Maurizio Del Greco has received fees from Abbott. The others authors reported no conflict of interests.

Abstract

BACKGROUND

This work dealt with the assessment of a computational tool to estimate the latest electrically activated segment (LEAS) of the left ventricle during cardiac resynchronization therapy (CRT).

OBJECTIVE

The aim of the work was to show that for patients with left bundle branch block (LBBB), possibly in presence of fibrosis, the proposed computational tool was able to accurately reproduce the electrical epicardial activation maps and in particular LEAS location in the coronary sinus (CS) branches.

METHODS

We considered a computational tool based on Finite Elements used to recover the electrical activation maps in all the myocardium. The model was calibrated by using activation times acquired in the CS branches with an electroanatomic mapping system (EAMS).

RESULTS

We applied our computational tool to predict electrical maps in the CS branches and LEAS for ten patients. We found an excellent accordance with EAMS measures, in particular the error for LEAS location was less than 4mm. We also calibrated our model using only the activation maps of the CS, still obtaining an excellent agreement with the measured LEAS.

CONCLUSION

We showed that our computational tool is able to accurately predict the electrical activation maps of the epicardial left ventricle surface also in cases with relevant fibrosis. In particular, we could estimate the location of LEAS, often used as a target site for the left lead placement during CRT, even when information only at CS were used for calibration.

KEYWORDS

Cardiac resynchronization therapy, latest electrically activated segment, computational models, epicardial veins, coronary sinus

Introduction

Cardiac resynchronization therapy (CRT) is an effective treatment for ventricular dyssynchrony (VD), which is often implicated in the development of congestive heart failure.[1] The main conduction disfunction which leads to VD is the left bundle branch block (LBBB). Despite improvements in recent years in CRT efficacy, the therapy has a non-responder rate of about 30%.[2] A possible way to improve CRT, in terms of clinical outcome and patient follow-up, consists in the optimal localization of the left lead. In recent years some attention has been paid on the latest electrically activated segment (LEAS) in the left ventricle (LV) as a target site for the left lead placement.[3,4] Measurements of LEAS require epicardial veins mapping by standard transvenous approach. A few years ago the use of the electroanatomical mapping system (EAMS) has been introduced also for the mapping of the coronary sinus (CS) and its branches.[4,5] Subsequent studies have shown how this approach can guide CRT implantation by indicating LEAS for lead placement. [6,7] However, this technique remains rather laborious and time consuming.

In the present work a new computational tool[8], validated in[9], is proposed for the estimation of LEAS. Our approach allowed us to obtain activation times in all the LV myocardium, thus providing, in particular, a complete “virtual mapping” of the epicardial veins. In particular, the computational model was calibrated by using activation measures in the CS branches obtained by EAMS. The aim of the work was to assess the accuracy of estimates provided by the model on patients with and without fibrosis. To this aim, we compared activation maps obtained by the computational model with those measured in the CS branches by means of

EAMS, with a particular focus on LEAS prediction. Moreover, we have repeated the same procedure to estimate LEAS by using only the points acquired at CS to calibrate our model.

Methods

This study was independent, non-industry-sponsored, and approved by the local ethical committee.

Patient-specific geometric reconstruction

Ten patients (P1-P10) affected by LBBB underwent a non-contrast enhanced cardiac and respiratory gated 3D MRI acquisition of both ventricles. A series of short-axis slices was acquired with a resolution of 2.34 × 2.34 mm^2 and slice thickness of 8 mm.

LV epicardium and endocardium surfaces were segmented using the open-source software MITK (http://www.mitk.org/wiki/MITK). A 3D interpolation has been applied to the short-axis images.

Using suitable meshing tools[10], we generated ten finite elements hexahedral volumetric meshes with mean edge length of 0.35 mm for each patient (Figure 1, right).

Bullseye division

The presence of fibrosis was revealed by MRI images in seven patients (P4-P10). Because of the low resolution, we could not properly reconstruct the fibrosis anatomy. However, starting to the standard 17-segment bullseye plots with the fibrosis distribution (Figure 1, left) we developed a tool able to split the reconstructed 3D geometry into 17 sub-volumes representing such segments (Figure 1, middle).

Electrical data and geometric alignment of computational geometry

For each patient an electroanatomic mapping of the coronary epicardial veins, in particular of CS branches, was performed by means of the *EnSite Precision* system[11] to record local activation times during the procedure to implant CRT.[4,5,7] In Table 1 the number of total measures N_{TOT} has been reported. Moreover, for P1-P5 we had also at disposal a mapping of the septum.

In order to merge electrical and geometric data we suitably projected all the electrical points on the epicardial surface of the LV geometry[9] (Figure 2).

Electrophysiological mathematical model

Cardiac electrophysiology (EP) in the LV patient-specific geometries was modeled by the monodomain equation coupled with the Bueno-Orovio ionic model.[12] For time discretization we used the forward Euler method for the ionic equation and a first order semi-implicit method for the monodomain equation.[9] The time step was $2.5*10^{-5}$s, a suitable value to capture the propagating front.[13]

For space discretization, we used linear Finite Elements on hexahedral meshes. All the computational framework has been implemented in *life*^{x} (https://lifex.gitlab.io/lifex), an academic high-performance C++ library for cardiac applications, based on the deal.II core.[14] When available (P1-P5), the septal data were used as input in the computational simulations. For the other cases (P6-P10) we prescribed as input the activation time in three selected points of the septum, according to standard observations made for LBBB patients.[15] The output of the computational simulations was the transmembrane potential at discrete temporal points (approximately 40 thousand per heartbeat) and at discrete spatial points, one for each vertex of the mesh. Starting from the trans-membrane potential, we computed the activation time for each discrete point as the discrete time instant where the trans-membrane potential has the highest variation rate.

Parameters estimation

The activation times measured at the CS branches were used as *calibrating data* to estimate the parameters in the monodomain equation, specifically the conductivities σ_f, σ_s, σ_n along the fibers, the sheets, and the normal directions, respectively. See[9] for further details. The conductivity values were differentiated to account for the different velocity of propagation in the three directions. For patients without fibrosis, these values were assumed to be constant in the whole myocardium, whereas for patients with fibrosis they were suitably reduced in the segments characterized by fibrosis, where conductivity is not necessarily zero as happens in presence of scars.[16] In order to properly select for each patient the values of the conductivities, we minimize the discrepancy at the epicardial veins between activation times obtained by computational simulations and those acquired by EAMS. This approach has been previously validated.[9]

In order to make our approach useful for the clinical practice, we repeated for five patients (P3,P4,P5,P8,P10) the estimation of conductivities by using as calibrating data only the measures acquired at CS (i.e. the most proximal ones). In Table 1 the number of measures N_{CS} at CS has been reported.

Reconstruction of the epicardial veins

We finally need to reconstruct the epicardial vein geometries, where the computational LEAS is evaluated. The MRI images at our disposal were not fine enough to allow the segmentation of such veins. Thus, we proposed here a method for their reconstruction. The idea was to exploit the locations of the points acquired by EAMS to draw the anatomy of the veins through the use of splines, an accurate mathematical tool widely used for interpolation e.g. in computer graphics.[17] For this purpose, we used the Paraview software, which allowed

us to manually manage the control points of the splines to improve the geometric reconstruction of the epicardial veins.

Prediction of the latest electrically activation segment: consistency test

In the CRT context, the clinical interest is focused on the point of the epicardial veins corresponding to the latest electrically activation segment (from now on *measured* LEAS), often used for the location of the left ventricular lead.[3,5-7]

Thanks to the computational pipeline described above and reviewed in Figure 2, we were able to solve the monodomain problem with the estimated conductivities and compute for each patient the activation times in the myocardial geometry. In particular, this allowed us to identify the *computational* LEAS*,* that is the point in the reconstructed veins featuring the latest activation segment among all the ones obtained by the computational simulations. This *consistency test* allowed us to assess the suitability of the computational model to accurately estimating measured LEAS. Moreover, we were also able to compute LEAS among all the points of the epicardium, not only those belonging to the veins *(computational global* LEAS*)*. This could be of particular interest when epicardial surgery procedure are used as an alternative to the standard transvenous technique.[18]

Prediction of the latest electrically activation segment: clinically relevant test

The previous estimation of computational LEAS and the comparison with measured LEAS have been performed for all the patients in the case when all the epicardial veins measures were used as calibration data. This procedure has been then repeated for patients P3, P4, P5, P8, P10 also in the case when only measures at CS were used as calibrating data, see Figure 2. In this case, we proposed to verify if our method was able to well predict LEAS by using only few data, in particular those at CS. This could provide a way to predict LEAS by using a shorter mapping procedure than the standard one. In particular, it might be enough

to map only the most accessible epicardial points (i.e. those at CS) to extract clinically relevant information about LEAS (*clinically relevant test*).

Results

Consistency test

In Figure 3 we reported the collection of geometric and electric data (in bullets) after their alignment[9], together with the continuous maps of activation times obtained by the computational simulations after calibration with all the epicardial veins measures. In Table 1 we reported (in black) the values of the conductivities estimated for each patient to match the measures. We observe values in the physiological ranges (0.7,2.2)x(0.16,0.48)x(0.03,0.1) $k\Omega^{-1}cm^{-1}$.[19-21]

In Figure 4 we show the computed trans-membrane potentials at three selected times. We can notice that for all the cases the first activated region is the septum. This is coherent with the electrical propagation in LBBB patients where the electrical signal enters the LV through the septum activated by the right ventricle. Notice from the corresponding bullseyes the lower velocity of propagation in the region with fibrosis.

From Figure 3, we observe a very good agreement between computations and measures. To provide a quantitative analysis, in Table 1 we report (in black) the errors obtained by our computational simulations. In particular, we computed the mean relative error and the standard deviation over the total number of measurements. We observe an excellent agreement between computational experiments and measures, the error being in any case less than 8%. In particular, for patients without fibrosis (P1-P3) the average error was 5.2%, whereas for the patients with fibrosis (P4-P10) it was 6.1%. This is not surprising, since in the latter case there are more parameters to determine (the conduction velocity being not constant).

In Figure 3 we showed also the reconstructed epicardial veins together with the position of measured LEAS, computational LEAS, and computational global LEAS. We notice an excellent agreement between the position of measured and computational LEAS. On the other side, the computational global LEAS is always quite far from the other two LEAS.

To go deeper in the analysis, in Table 2 we reported the values of the distance D1 (intended as the geodesic distance over the epicardial surface) between measured and computational LEAS. These results confirmed the great ability of the computational tool in predicting LEAS, the error in terms of distance being in any case less than 0.41 cm (average 0.23 cm). D1 assumed an average value of 0.27 cm for P1-P3 (that is for patients without fibrosis) and of 0.21 cm for P4-P10 (that is for patients with fibrosis), highlighting that the accuracy of the computational tool in predicting the location of LEAS is independent of the presence of fibrosis.

Also, we reported the distance D2 between measured LEAS and computational global LEAS, and the difference Δ_{AT} between the activation times corresponding to these segments. We observe significant values of the distance which is in any case greater than 1.73 cm, reaching values up to more than 5 cm (average 3.15 cm). This means that if we are looking for the point with the absolute largest activation time over all the epicardial surface (thus not restricting our search in the epicardial veins), we would find points quite far from measured and computational LEAS. However, the delay in terms of activation time with respect to measured LEAS is in average 14.6 ms, therefore only about 10% of the global duration of the QRS.

Clinically relevant test

In the second test, we assessed the accuracy of the computational LEAS predicted by computational simulations calibrated by using only measures acquired at CS, that is the most proximal ones. In Figure 5, we reported the corresponding location of LEAS together

with the continuous computational map of activation times and the reconstructed epicardial veins.

In Table 1 we reported in the second column of each box (when available, in red) the values of the estimated conductivities together with the relative error (obtained against all the measures at disposal, not only those at CS) and the standard deviation. From these results, we observe that the conductivity values estimated by using only the measures at CS are very similar to those of consistency test, where all the measures were used for calibration. Accordingly, we observe a very small increment of the relative error with respect to the consistency test.

In view of the clinical validity of this test, in Table 2 we reported in the second column of each box (when available, in red) the values of the distances D1 and D2. In particular, D1 resulted to be the same of the consistency test for four of the five patients, whereas it was a little bit larger for one case. As for D2, again the values are very similar to the consistency test. We also reported the differences Δ_{AT} between activation times of measured LEAS and computational global LEAS, which feature exactly the same values obtained by the consistency test.

Discussion

Computational methods represent nowadays a very promising, non-invasive tool to provide clinical indications in different applications of electro-physiology. In particular, there is in the literature a growing interest in using computational models to predict and support the clinical practice for CRT.[22-25]

In this work, we have used a computational method, previously validated for non-fibrotic cases[9], to 10 LBBB cases (3 without fibrosis, 1 with moderate fibrosis, and 6 with wide fibrosis) with the aim of predicting the electrical activation maps in the CS branches. The error between computations and measures obtained by EAMS was in any case less than

8% showing the accuracy of our tool, which is able to reproduce a complete myocardial activation map (Figure 3, left). This could be thought as the first step towards the modeling of the processes that are at the basis of intraventricular conduction disorders.

More specifically, we focused on the prediction of LEAS, which has been seen to be an optimal site for the location of the left lead during CRT.[3,4] Our results showed that the distance between LEAS mapped during EAMS by cardiologists and those predicted by our computational model is in any case less than 4mm (Table 2), indicating the great ability of our tool to well predict LEAS location.

More interestingly, we showed for 5 cases (1 without fibrosis and 4 with fibrosis) that it is enough to know the activation times at CS to well predict the location of LEAS in the CS branches. This result could be of utmost importance in view of a possible clinical application. Indeed, previous studies have suggested that left ventricular pacing in a site with late activation (either mechanical or electrical), rather than anatomically pre-specified left ventricular segments, may improve the hemodynamic response, reverse remodeling, and clinical outcome of patients underwent to CRT implantation.[3,26-28] Our group demonstrated that EAMS-guided CRT implantation is a safe, reliable and effective technique that provides useful information on the electrical activation of CS and its branches in order to guide the placement of the left ventricular lead.[4-7] Also, it demonstrated that there was a strong correlation between CS-LEAS and branches-LEAS: in other words, from the CS regions of highest activation delay, origins the vessel with highest activation delay; this finding can reduce procedural time during CRT implant, with or without EAMS, by limiting the search of the target vessel for left ventricular lead placement to the CS area with the largest delay.[29] Several studies have investigated the presence and variability of CS tributaries.[30,31] These anatomical structures are characterized by high anatomic, location and course interpatient variability.[32] The possibility of predicting the site of highest delay in the LV with a mathematical model with the acquisition of a few points in CS could facilitate the mapping

procedure, providing a potential benefit for patients, and the overall implantation of a CRT device, possibly promoting improvements in the number of patients responding to therapy,

This evaluation would also be useful to discriminate those patients in which there is no vein in the delayed area to evaluate whether to submit them to alternative resynchronization techniques, e.g. implantation of CRT with epicardial catheter for stimulation of the LV in minithoracotomy.[33] Nowadays the epicardial surgery is not only employed in patients with failed CS left ventricular lead implantation but also as an alternative to the standard transvenous technique.[18] With this respect, the possibility to compute LEAS among all the epicardial points (and not only those in the veins) by means of a computational model (computational global LEAS) as described in this work provides a reliable way to localize an effective location for the left catheter implantation during minithoracotomy.

Despite these promising results, we are still far to concretely propose our method for an implementation in the current mapping devices. This because of the high computational times still requested to solve the related electrophysiology problems to determine maps of activation times and in particular LEAS, even using clusters of high performing computers. We are working in this direction in order to reduce the computational effort of our strategy and to make it close to real time. In this direction, we are exploring different mathematical models which are less accurate but much faster, such as the Eikonal model.[8,25,34]

In any case, we believe that the results presented in this work could represent a first step towards the inclusion of a computational tool in an electrophysiology mapping device in order to shorten the invasive procedure and give an effective support in determining activation maps and in particular LEAS position.

Conclusions

In this work we have used a computational tool for the prediction of myocardial electrical activation maps and in particular of the location of LEAS in the CS branches, usually determined by means of a mapping procedure and used for CRT implantation. The model

was calibrated by using the activation maps obtained by EAMS navigating CS branches. Its application to ten patients with LBBB and possible fibrosis showed an excellent agreement between computational and measured activation maps and LEAS. Remarkably, for five of the ten patients we showed that it was enough to use activation maps only at CS to calibrate the model in order to well predict LEAS in the CS branches.

These results provide a first preliminary step towards the use of computational tools to better understand the conditions that could lead to intraventricular conduction disorders and to assist CRT by providing a support and simplification of EAMS.

References

[1] Bax JJ, Bleeker GB, Marwick TH, et al. Left ventricular dyssynchrony predicts response and prognosis after cardiac resynchronization therapy. Journal of the American College of Cardiology 2004, 44(9):1834-1840.

[2] Kass DA. Ventricular resynchronization: Pathophysiology and identification of responders. Reviews in Cardiovascular Medicine 2003, 4(SUPPL. 2), S3-S13.

[3] Liang Y, Yu H, Zhou W, et al. Left Ventricular Lead Placement Targeted at the Latest Activated Site Guided by Electrophysiological Mapping in Coronary Sinus Branches Improves Response to Cardiac Resynchronization Therapy. Journal of Cardiovascular Electrophysiology 2015, 26(12):1333–1339.

[4] Del Greco M, Marini M, Bonmassari R. Implantation of a biventricular implantable cardioverter-defibrillator guided by an electroanatomic mapping system. Europace 2012,14(1):107-11.

[5] Del Greco M, Maines M, Marini M, et al. Three-Dimensional Electroanatomic Mapping System-Enhanced Cardiac Resynchronization Therapy Device Implantation: Results From a Multicenter Registry. Journal of Cardiovascular Electrophysiology 2017, 28(1):85-93.

[6] Rad MM, Blaauw Y, Dinh T, Pison L, Crijns HJ, Prinzen FW, Vernooy K. Left ventricular lead placement in the latest activated region guided by coronary venous electroanatomic mapping. Europace 2015,17(1):84-93

[7] Del Greco M, Zorzi A, Di Matteo I, Cima A, Maines M, Angheben C, Catanzariti D. Coronary sinus activation patterns in patients with and without left bundle branch block undergoing electroanatomic mapping system-guided cardiacresynchronization therapy device implantation. Heart Rhythm 2017,14(2):225-233.

[8] Quarteroni A, Manzoni A, Vergara C. The cardiovascular system: mathematical modelling, numerical algorithms and clinical applications. Acta Numerica 2017, 26:365-590.

[9] Stella S, Vergara C, Maines M, et al. Integration of activation maps of epicardial veins in computational cardiac electrophysiology. Computer in Biology and Medicine 2020, 127, 104047.

[10] Fedele M. Polygonal surface processing and mesh generation tools for numerical simulations of the complete cardiac function. MOX Report 32, Politecnico di Milano, 2019.

[11] Eitel C, Hindricks G, Dagres N, Sommer P, Piorkowski C. EnSite Velocity™ cardiac mapping system: a new platform for 3D mapping of cardiac arrhythmias. Expert Rev Med Devices 2010,7(2):185–192.

[12] Bueno-Orovio A, Cherry EM, and Fenton FH. Minimal model for human ventricular action potentials in tissue. Journal of Theoretical Biology 2008, 253(3):544-560.

[13] Gurev V, Lee T, Constantino J, Arevalo H, and Trayanova NA. Models of cardiac electromechanics based on individual hearts imaging data. Biomechanics and Modeling in Mechanobiology 2010, 10(3):295-306.

[14] Arndt D, Bangerth W, Clevenger TC, et al. The deal.II library, version 9.1. Journal of Numerical Mathematics 2019, 27(4):203-213.

[15] Strik M, Regoli F, Auricchio A et al. Electrical and Mechanical Ventricular Activation During Left Bundle Branch Block and Resynchronization. Journal of Cardiovascular Translational Research 2012, 5:117–126.

[16] Coronel R, Casini S, Koopmann TT, et al. Right ventricular fibrosis and conduction delay in a patient with clinical signs of Brugada syndrome: a combined electrophysiological, genetic, histopathologic, and computational study. Circulation, 2005, 112(18):2769-2777.

[17] Quarteroni A, Sacco R, Saleri F, Numerical Mathematics, Springer, Berlin, 2000.

[18] Navia JL, Atik FA, Grimm RA, et al. Minimally invasive left ventricular epicardial lead placement: surgical techniques for heart failure resynchronization therapy. Annals of Thoracic Surgery 2005, 79(5):1536-1544.

[19] Clerc L. Directional differences of impulse spread in trabecular muscle from mammalian heart. The Journal of Physiology 1976, 255(2):335-346.

[20] Stinstra JG, Hopenfeld B, and MacLeod RS. On the passive cardiac conductivity. Annals of Biomedical Engineering 2005, 33(12):1743-1751.

[21] Le Guyader P, Trelles F, and Savard P. Extracellular measurement of anisotropic bidomain myocardial conductivities. i. theoretical analysis. Annals of Biomedical Engineering 2001, 29(10):862-877.

[22] Hyde ER, Behar JM, Claridge S, et al. Beneficial Effect on Cardiac Resynchronization From Left Ventricular Endocardial Pacing Is Mediated by Early Access to High Conduction Velocity Tissue. Circulation: Arrhythmia and Electrophysiology 2015, 8(5), 1164–1172.

[23] Mendonca Costa C, Neic A, Kerfoot E, et al. Pacing in proximity to scar during cardiac resynchronization therapy increases local dispersion of repolarization
and susceptibility to ventricular arrhythmogenesis. Heart Rhythm 2019, 16(10):1475–1483.

[24] Mendonca Costa C, Neic A, Gillette K, et al. Left ventricular endocardial pacing is less arrhythmogenic than conventional epicardial pacing when pacing in proximity to scar. Heart Rhythm 2020, 17(8), 1262–1270.

[25] Lee AWC, O'Regan DP, Gould J, et al. Sex-Dependent QRS Guidelines for Cardiac Resynchronization Therapy Using Computer Model Predictions. Biophysical Journal 2020, 117(12), 2375–2381.

[26] Zanon F, Baracca E, Pastore G, Fraccaro C, Roncon L, Aggio S, Noventa F, Mazza A, Prinzen F. Determination of the longest intrapatient left ventricular electrical delay may predict acute hemodynamic improvement in patients after cardiac resynchronization therapy. Circ Arrhythm Electrophysiol. 2014;7:377-83.

[27] Ypenburg C, van Bommel RJ, Delgado V, Mollema SA, Bleeker GB, Boersma E, Schalij MJ, Bax JJ. Optimal left ventricular lead position predicts reverse remodeling and survival after cardiac resynchronization therapy. J Am Coll Cardiol. 2008;52:1402-9.

[28] Gold MR, Birgersdotter-Green U, Singh JP, Ellenbogen KA, Yu Y, Meyer TE, Seth M, Tchou PJ. The relationship between ventricular electrical delay and left ventricular remodelling with cardiac resynchronization therapy. Eur Heart J. 2011;32:2516-24.

[29] Maines M, Peruzza F, Zorzi A, Moggio P, Angheben C, Catanzariti D, Coletti M, Pangrazzi C, Del Greco M. Coronary sinus and great cardiac vein electroanatomic mapping predicts the activation delay of the coronary sinus branches. J Cardiovasc Electrophysiol. 2020 Jun 11. doi: 10.1111/jce.14609. Epub ahead of print. PMID: 32525574.

[30] Jongbloed MR, Lamb HJ, Bax JJ, et al. Noninvasive visualization of the cardiac venous system using multislice computed tomography. J Am Coll Cardiol. 2005;45:749-753.

[31] Boonyasirinant T, Halliburton SS, Schoenhagen P, Lieber ML, Flamm SD. Absence of Coronary Sinus Tributaries in Ischemic Cardiomyopathy: An Insight from Multidetector Computed Tomography Cardiac Venographic Study. Journal of Cardiovascular Computed Tomography. 2016;10(2):156-161.

[32] Ortale JR, Gabriel EA, Iost C, et al. The anatomy of the coronary sinus and its tributaries. Surg Radiol Anat 2001;23:15–21.

[33] Sieniewicz BJ, Gould J, Porter B, Sidhu BS, Teall T, Webb J, Carr-White G, Rinaldi CA. Understanding non-response to cardiac resynchronisation therapy: common problems and potential solutions. Heart Fail Rev. 2019;24(1):41-54.

[34] Palamara S, Vergara C, Catanzariti D, Faggiano E, Centonze M, Pangrazzi C, Nobile F, Maines M, Quarteroni A, Computational generation of the Purkinje network driven by clinical measurements: The case of pathological propagations. Int. J. Num. Meth. Biomed. Eng. 2014;30(12):1558-1577.

	N_{TOT} / N_{CS}	σ_f	σ_s	σ_n	Mean relative error (%)	Std (%)
P1	39	1.57	0.41	0.08	3.55	2.02
P2	32	1.23	0.25	0.07	4.97	2.68
P3	33 / 8	1.39 / 1.41	0.30 / 0.31	0.07 / 0.07	5.32 / 5.94	1.95 / 1.96
P4	32 / 7	1.38 / 1.42	0.67 / 0.71	0.07 / 0.08	5.67 / 6.23	2.21 / 2.35
P5	84 / 10	1.36 / 1.32	0.54 / 0.51	0.08 / 0.08	4.53 / 5.32	1.83 / 2.08

P6	25	1.25	0.51	0.06	5.30	2.29
P7	17	1.32	0.55	0.07	5.13	2.76
P8	20 / 7	1.21 / 1.23	0.39 / 0.42	0.06 / 0.07	7.96 / 8.74	2.61 / 2.95
P9	48	1.28	0.28	0.06	6.89	3.11
P10	86 / 10	1.31 / 1.28	0.30 / 0.28	0.07 / 0.06	3.24 / 4.15	1.53 / 1.86

Table 1. Number of measures, conductivities, errors.

Number of total (N_{TOT}) and coronary sinus (N_{CS}) measurements used for calibration; Values of estimated conductivities σ_f, σ_s, σ_n; Mean relative error with standard deviation. In black: consistency test. In red, when available: clinically relevant test.

	D1 (cm)	**D2 (cm)**	**Δ_{AT} (ms)**
P1	0.26	3.71	15
P2	0.35	3.06	15
P3	0.21 / 0.21	1.96 / 1.95	11 / 11
P4	0.16 / 0.16	1.95 / 1.96	12 / 12
P5	0.11 / 0.13	1.73 / 1.76	11 / 11
P6	0.41	2.89	15
P7	0.24	5.22	20
P8	0.09 / 0.09	1.53/ 1.52	8 / 8

P9	0.38	5.65	19
P10	0.08 / 0.08	3.75 / 3.74	20 / 20

Table 2. Distances between measures and computations

Distance D1 between measured and computational LEAS; Distance D2 between measured and computational global LEAS; Difference Δ_{AT} between activation times of measured and computational global LEAS. In black: consistency test. In red, when available: clinically relevant test.

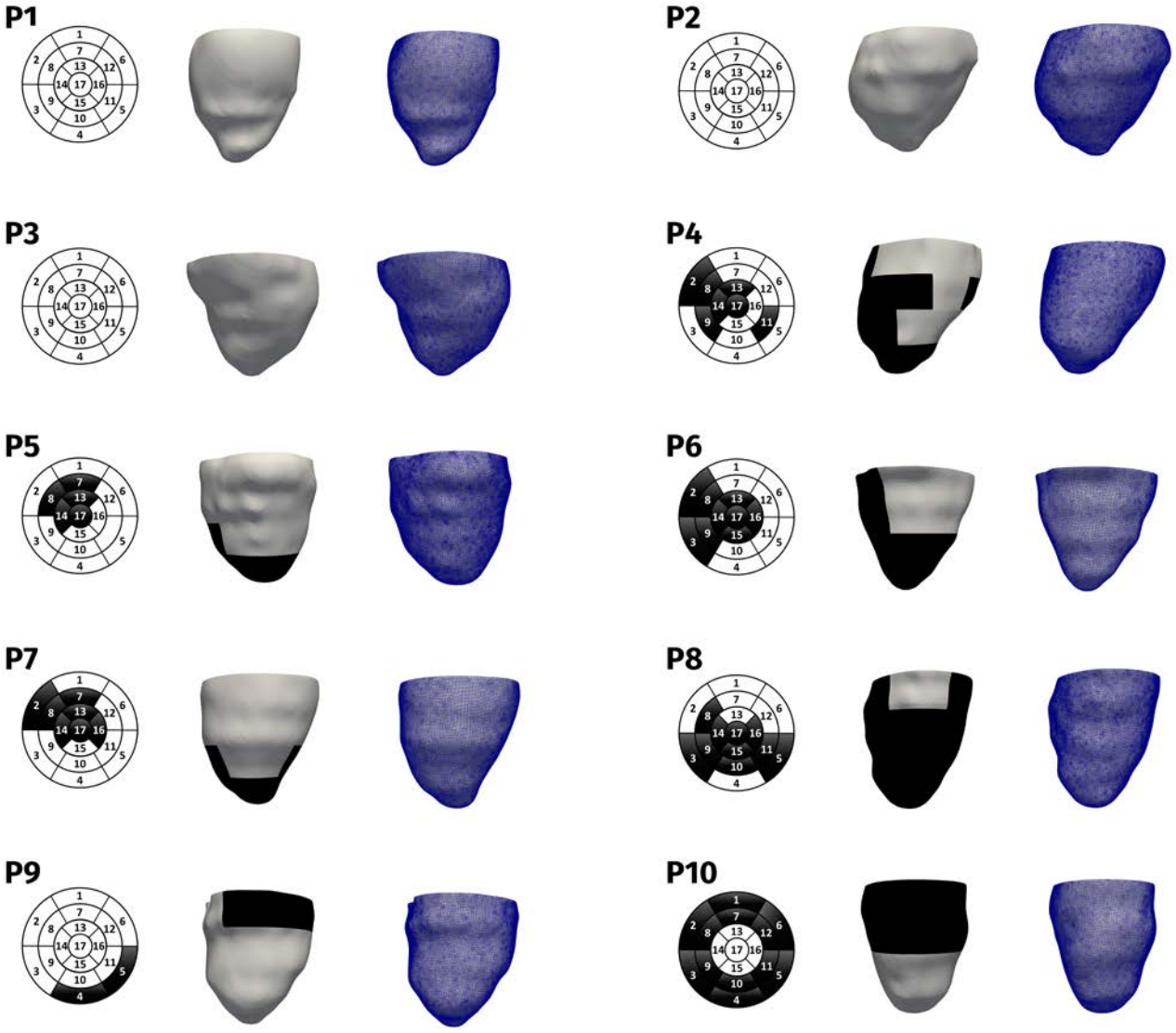

Figure 1. Bullseyes, geometries, and computational meshes

Left: bullseye plot of the fibrotic distribution. Middle: front perspective of the reconstructed geometry subdivided into fibrosis (black) and healthy tissue (white). Right: computational mesh (for visualization purposes, a coarser one with respect to the one used in simulations).

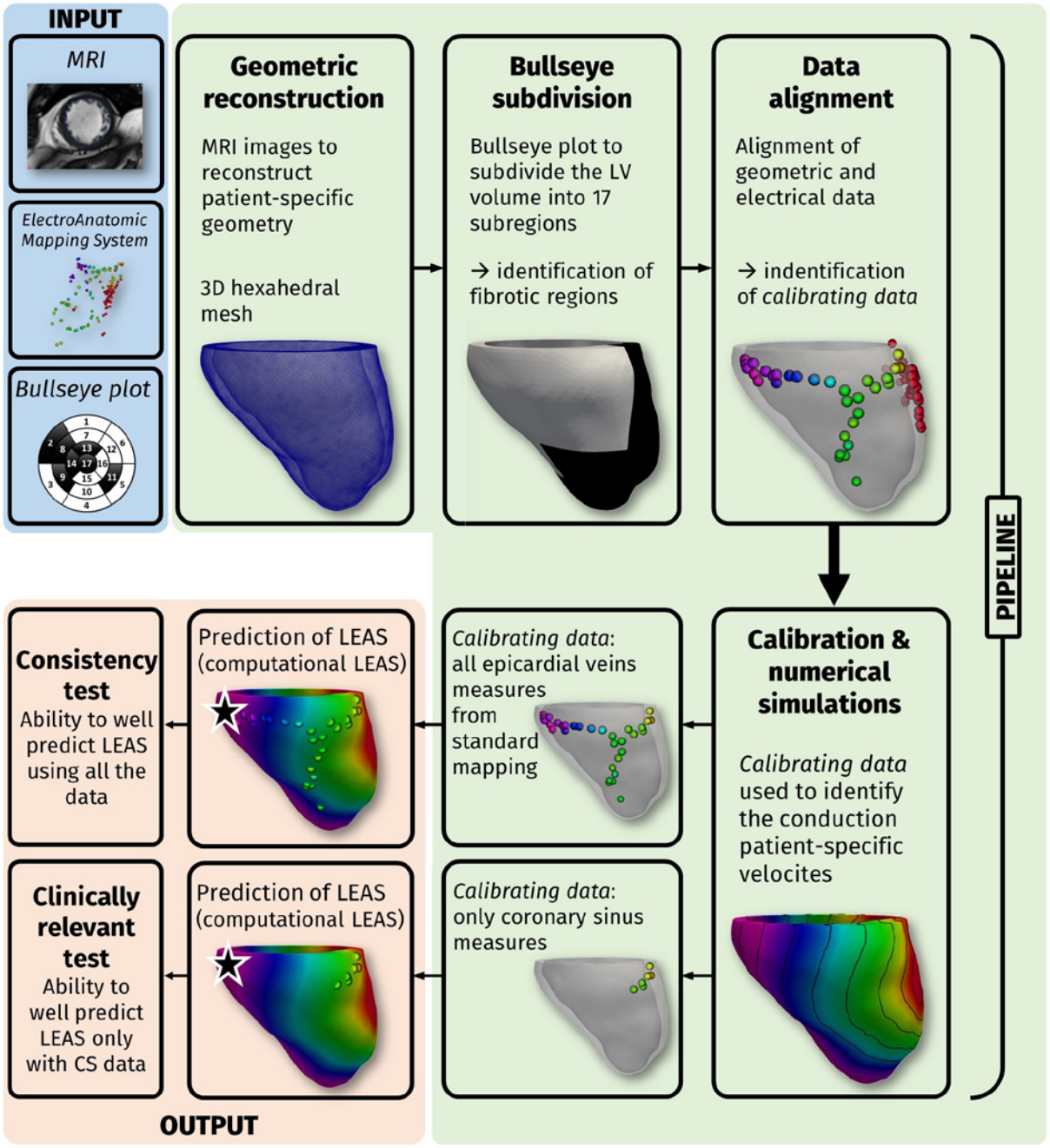

Figure 2. Workflow

Inputs (in light blue): MRI images, electroanatomic measures and bullseye plots; Pipeline steps (in green): geometric reconstruction of the LV; bullseye subdivision; alignment of geometric and electrical data; calibration and computational results of activation time; choice of *calibrating data*: i) all measures at the epicardial veins (consistency test); ii) measures only at the coronary sinus (clinically relevant test);

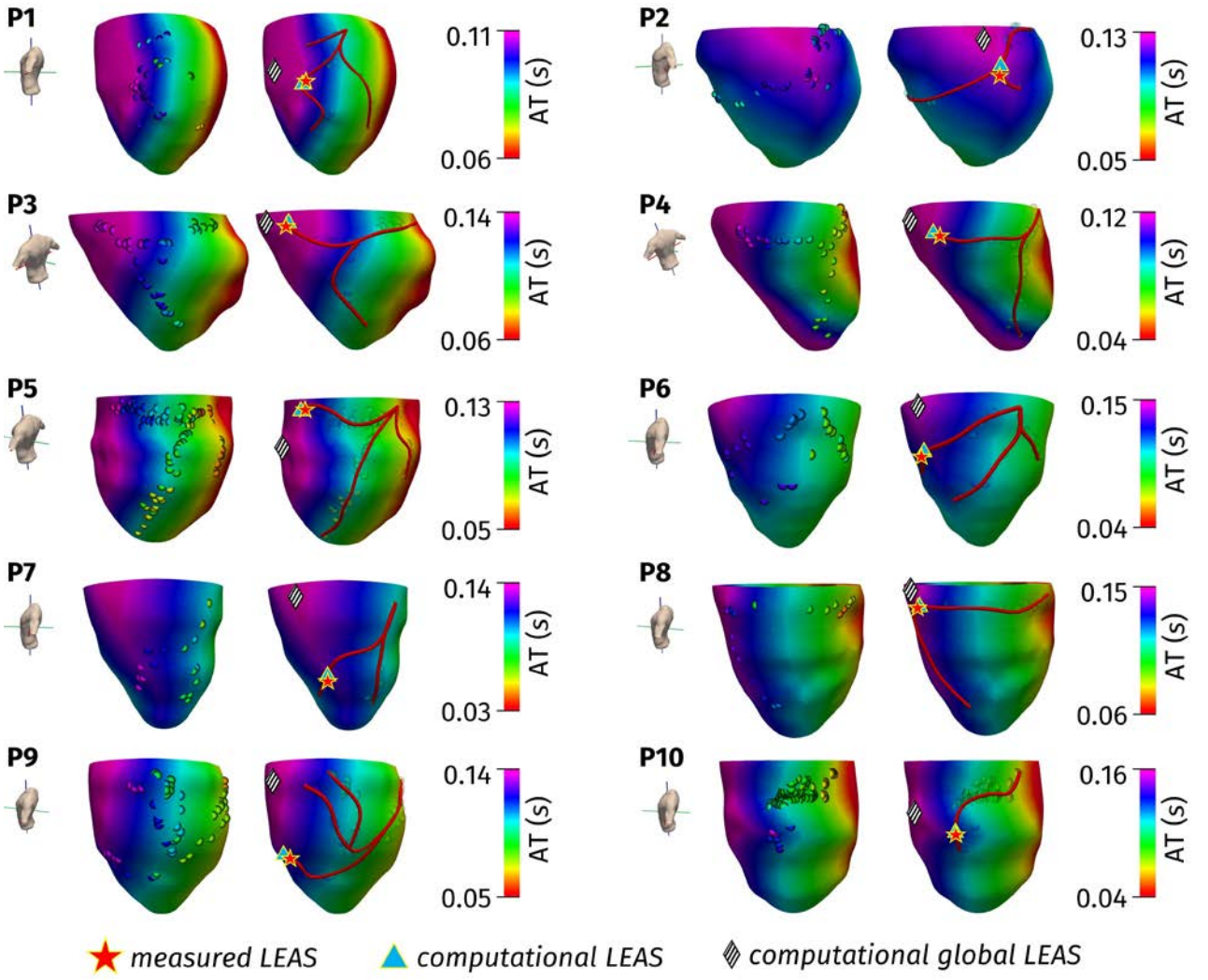

Figure 3. Measured and computed activation maps. Consistency test.

Left: Computed (continuous map) and measured (bullets) activation times. Right: Reconstructed epicardial veins (in red) and location of LEAS.

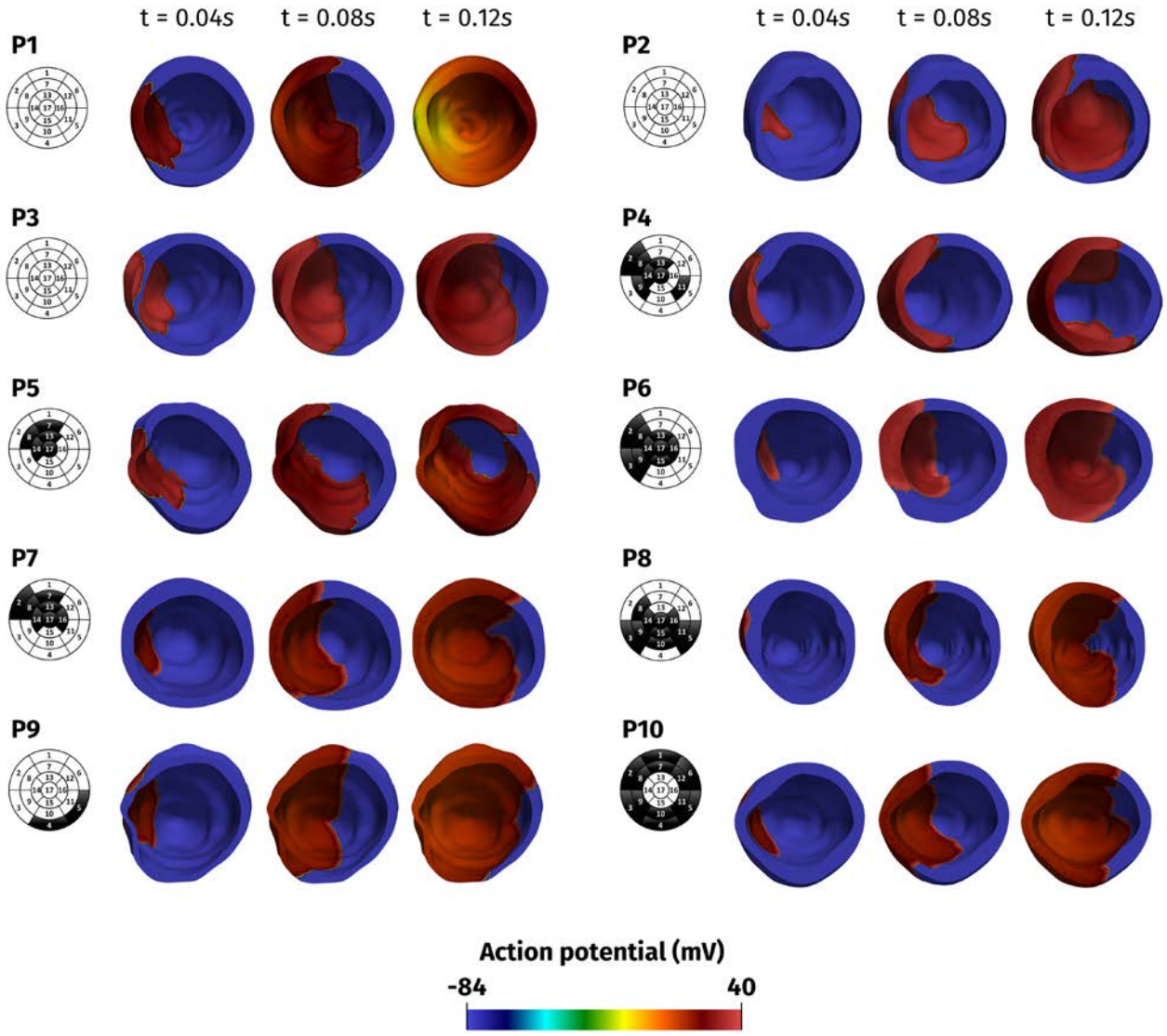

Figure 4. Maps of electrical potential

Maps of electrical potential at three instants together with bullseye plot. Consistency test.

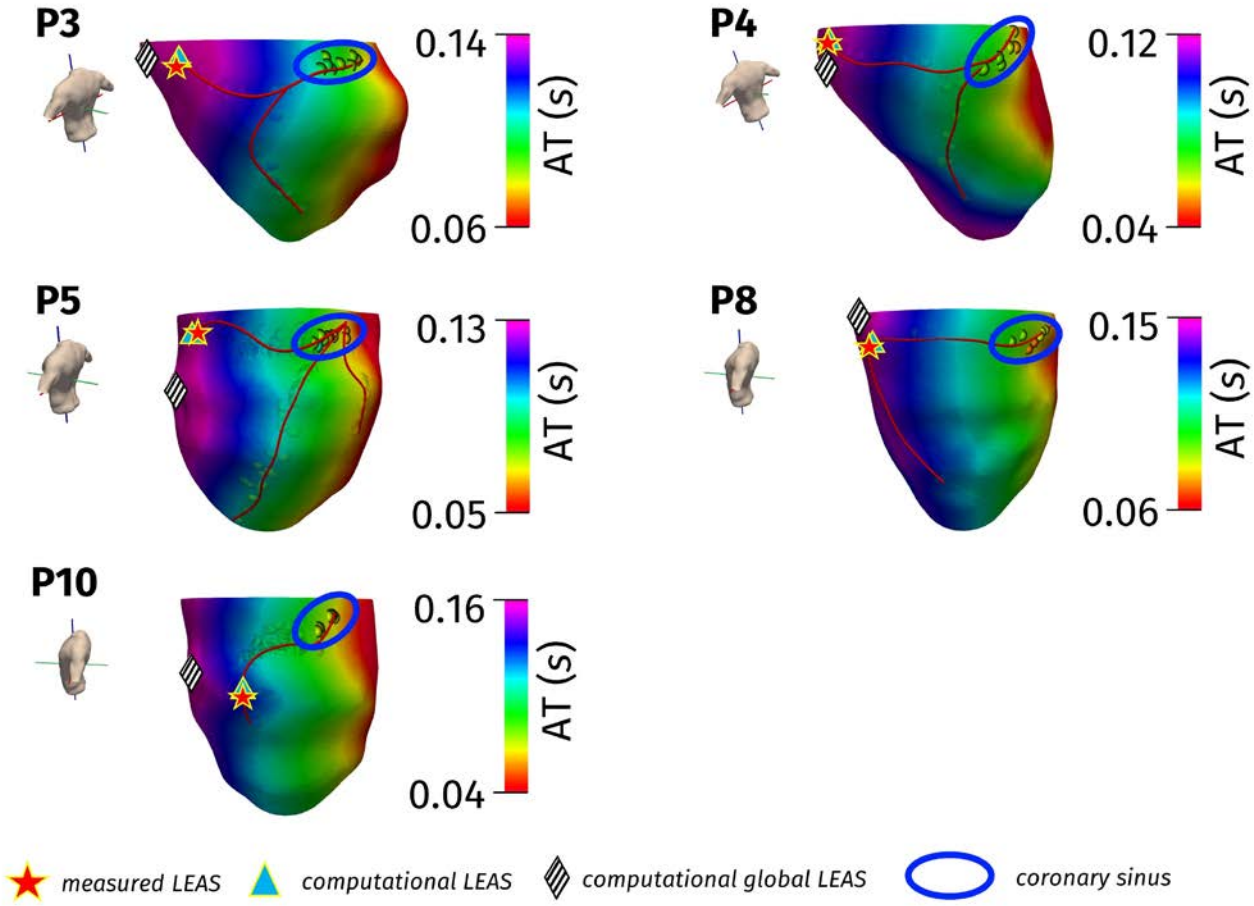

Figure 5. Measured and computed activation maps. Clinically relevant test.

Computed (continuous) activation maps, measurements of activation time in the coronary sinus (rounded in blue), reconstructed epicardial veins (in red) and locations of LEAS.